BioMedical Engineering OnLine

RESEARCH

Open Access

Effect of microtextured titanium sheets using laser enhances proliferation and collagen synthesis of mouse fibroblasts via the TGF-β/Smad pathway

Haoyu He[1†], Peiyao Wang[1†], Zhuo Liu[1,2†], Rongchuan Feng[3], Bang Liu[1], Qiang Song[1,4], Yahui Hu[3*] and Weihua Fu[1*]

[†]Haoyu He, Peiyao Wang and Zhuo Liu have contributed equally to this work.

*Correspondence: huyahuilg@126.com; tjmughgs_fwh@163.com

[1] Department of General Surgery, Tianjin Medical University General Hospital, 154 Anshan Road, Tianjin 300052, People's Republic of China
[2] Present Address: Department of General Surgery, Shijingshan Hospital, Shijingshan Teaching Hospital of Capital Medical University, Beijing, China
[3] Tianjin Key Laboratory of Advanced Mechanical and Electrical System Design and Intelligent Control, National Experimental Teaching Demonstration Center for Mechanical and Electrical Engineering, Tianjin University of Technology, No.391, Binshui West Road, Xiqing District, Tianjin, China
[4] Department of General Surgery, Baotou Central Hospital, Baotou 0140, Inner Mongolia, China

Abstract

Purpose: This study investigates the effects of hexagonal microtextured titanium sheets on fibroblast growth and collagen synthesis, crucial factors in anastomotic healing.

Materials and methods: Hexagonal titanium sheets were fabricated using a laser microtextured machine. Mouse fibroblastic embryonic stem cells (NIH/3T3) were cultured on these sheets. Cell proliferation was assessed using a CCK8 assay, and expression of TGF-β/Smad pathway-related genes and collagen types I and III was evaluated through qRT-PCR and western blot.

Results: Hexagonal titanium sheets significantly enhanced fibroblast growth and collagen synthesis. The 50–30 group, with the smallest contact angle (48 ± 2.3°), exhibited the highest cell growth rates by CCK8 assay. Gene expression analysis revealed that TGF-β1, Smad2, Smad3, Smad4, and COL1A1 were significantly upregulated in the 50–30 group on day 7. Meanwhile, type I collagen expression was significantly increased in the 50–30 group on day 7 by western blot analysis.

Conclusion: Our findings demonstrate that laser-fabricated hexagonal microtextured titanium sheets enhance hydrophilicity and promote fibroblast growth, activating the TGF-β/Smad pathway to facilitate collagen synthesis. These results have important implications for tissue repair and regeneration.

Keywords: Laser microtextured surface, Titanium, Fibroblast cells, Cell proliferation, Collagen secretion, Tissue repair

Introduction

The quality of anastomotic healing is a critical factor in assessing the success and prognosis of gastrointestinal (GI) surgery, as it is closely associated with surgical outcomes and the short- and long-term prognosis of patients [1]. With the development of minimally invasive surgical technique, instrumented anastomosis has been widely

used in gastrointestinal surgical procedures. At present, pure titanium or titanium–nickel alloy are the most frequently used clinical materials for gastrointestinal anastomotic staples due to pure titanium's ability to reduce inflammatory response, good biocompatibility, corrosion resistance, and low Young's modulus [2, 3]. While instrumented anastomosis enhances the quality of the anastomosis to some extent compared to traditional manual anastomosis, pure titanium, being an inert material, does not actively contribute to the healing process.

The healing of GI tissues occurs in three phases: the inflammatory phase, proliferative phase, and remodeling phase [4]. During this dynamic process, positively regulating the proliferation of tissue healing-related cells and increasing collagen secretion may enhance the tensile strength of the anastomosis. Given that anastomotic healing is primarily associated with the growth of fibroblasts and the synthesis of collagen fibers in the submucosal layer, some scholars have suggested enhancing fibroblast growth and collagen fiber synthesis by applying chemical coatings to the surface of anastomotic nails. For instance, Wang et al. [5] implanted a polylactic acid–acetic acid (PLGA)-coated scaffold containing 1 mg of doxycycline into the lumen of a colonic anastomosis to potentially prevent colonic leakage. Similarly, Chua et al. [6] deposited polyelectrolyte multilayers (PEMs) consisting of hyaluronic acid and chitosan on the surface of titanium implants to inhibit microbial adhesion and confer antimicrobial properties to the titanium implants. Nonetheless, the durability of surface coatings and their gradual degradation over time present challenges for the method of adding chemical coatings to implant surfaces. Furthermore, the effects of artificial implant materials on tissue healing have been investigated in the field of orthopedics. Prior research has demonstrated that artificial implant materials can markedly enhance angiogenesis and bone tissue healing [7, 8]. This indicates that biomechanics may be a pivotal factor in the process of tissue healing.

However, insufficient attention has been given to the staple's surface morphology despite the potential of changes in biomechanics to stimulate cell growth [9]. It may be critical to understand how the physical morphology of staples can convert mechanical signals into biological signals to promote wound healing. Among the myriad of signaling pathways involved, the transforming growth factor-beta (TGF-β) signaling pathway plays a critical role in orchestrating the processes of re-epithelialization, inflammation, angiogenesis, and granulation tissue formation [10]. Upon tissue injury, TGFβ is released from platelets and other cells, initiating a cascade of cellular activities that promote the migration and proliferation of fibroblasts and keratinocytes. This pathway facilitates the deposition of extracellular matrix components and enhances vascularization, both of which are vital for successful wound closure. The objective of this study was to investigate the impact of microtextured titanium surfaces on the TGF-β signaling pathway in fibroblasts.

In our study, we constructed hexagonal microtextured titanium sheets surface by laser microtextured marking technology. Our objective is to investigate the role of hexagonal microtextured titanium sheet surfaces in facilitating cell proliferation and tissue regeneration by converting mechanical signals on the surface of microtextured titanium sheets into bioelectrical signals within fibroblasts. The findings indicated that hexagonal microtextured titanium sheets significantly stimulate fibroblast

growth and collagen synthesis, highlighting their potential as a novel anastomotic staple for gastrointestinal anastomosis.

Results

The 50–30 group has the smallest surface contact angle, indicating that it has the best hydrophilicity

The hydrophilicity of each group of microtextured surfaces was determined by measuring their average roughness and contact angles. Good hydrophilicity favors cell growth. The average roughness (Ra) and the contact angles were measured in accordance with the previously described methodology. The statistical analysis revealed notable variations in the mean surface roughness among the polished group, 50–30 group, 50–90 group, and 150–30 group ($\boldsymbol{p} < 0.05$) (Table 1). Similarly, the mean surface contact angles exhibited significant differences among the polished, 50–30, 50–90, and 150–30 groups ($\boldsymbol{p} < 0.05$). It is noteworthy that the surface contact angle of the 50–30 group was the smallest, measuring $48 \pm 2.3°$, with a statistically significant difference ($\boldsymbol{p} < 0.01$). The aforementioned outcomes indicated that the 50–30 group might exhibit the most hydrophilic properties.

The microtextured titanium sheets surface promoted mouse fibroblast proliferation

To measure the viability of cells, CCK8 was performed as described before. The viability of cells in the experimental groups at day 0 was found to be statistically indistinguishable, indicating the absence of any significant artificial interference (Fig. 1). Notably, the 50–30 group exhibited the highest optical density (OD) value relative to the other groups. At days 2, 3, and 6, the OD of the 50–30 group was found to be significantly different from that of the second-highest group, 150–30. (1.3755 ± 0.0325 vs. 1.2509 ± 0.0047, $p < 0.01$; 2.2171 ± 0.0318 vs. 1.2702 ± 0.0188, $p < 0.0001$; 2.7804 ± 0.1443 vs. 2.5148 ± 0.0613, $p < 0.05$, respectively) (Table 2). Conversely, at the second and fourth days, the mouse fibroblasts in the 50–90 group exhibited significantly lower OD values than those in the polished group. (0.9644 ± 0.0085 vs. 1.0930 ± 0.0132, $\boldsymbol{p} < 0.001$; 1.8718 ± 0.0834 vs. 2.1787 ± 0.1048, $p < 0.05$, respectively). The results indicated that these discrepancies might be attributed to the compatibility of cell size with edge spacing on microtextured surface.

Table 1 Measured surface roughness and contact angle of each group of titanium sheets

	n	Surface roughness(μm)	Surface contact angle(°)
Polished	4	0.164 ± 0.05	65.5 ± 3.1
50–30	4	3.049 ± 0.32	48 ± 2.3
50–90	4	3.986 ± 0.31	57 ± 2.5
150–30	4	1.993 ± 0.18	61 ± 2.7

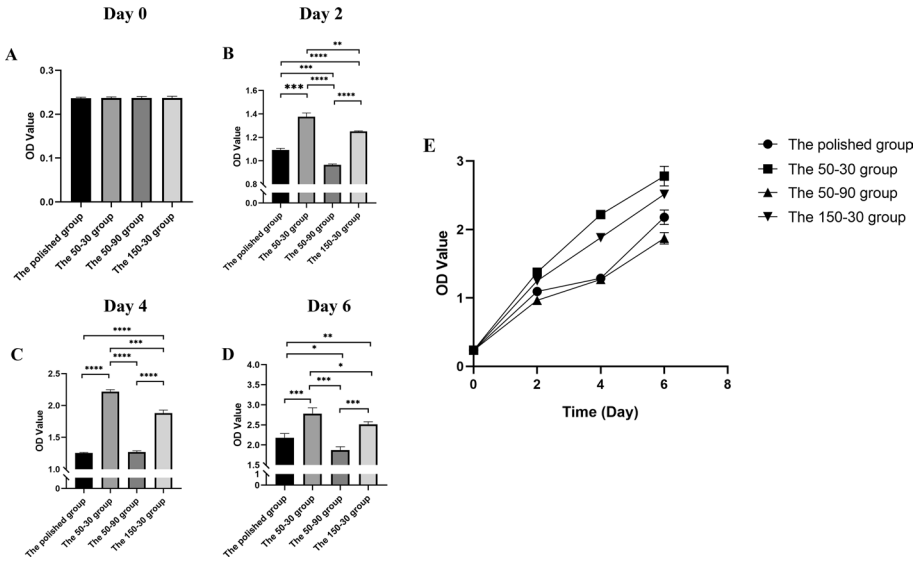

Fig. 1 Absorbance values of culture supernatants on titanium wafers: **A**–**D** absorbance at days 0, 2, 4, and 6 for each group; E dynamic changes from days 0 to 6. *$p < 0.05$, **$p < 0.01$, ***$p < 0.001$, ****$p < 0.0001$

Table 2 Absorbance values of culture supernatants on the surface of each group of titanium plates

	Day 0	Day2	Day 4	Day 6
Polished	0.2365 ± 0.0022	1.0930 ± 0.0132	1.2538 ± 0.0096	2.1787 ± 0.1048
50–30	0.2369 ± 0.0039	1.3755 ± 0.0325	2.2171 ± 0.0318	2.7804 ± 0.1443
50–90	0.2370 ± 0.0033	0.9644 ± 0.0085	1.2702 ± 0.0188	1.8718 ± 0.0834
150–30	0.2369 ± 0.0039	1.2509 ± 0.0047	1.8791 ± 0.0487	2.5148 ± 0.0613

Microtextured titanium sheets surface increased RNA expression of the TGF-β/SMAD pathway and COL1A1 and COL3A1 in mouse fibroblasts

The expression levels of genes related to collagen secretion were analyzed using quantitative real-time PCR (qRT-PCR), as described previously. On the fourth day of incubation, it was observed that the expression of COL1A1 and COL3A1 was significantly higher in all three microtextured groups compared to the polished group (Fig. 2) (Table 3). The findings indicated that the microtextured surface may have facilitated the secretion of collagen-related genes. Nevertheless, no statistically significant difference was observed in the expression of SMAD genes. On the seventh day of the experiment, the results were found to be highly promising. In particular, the expression levels of TGF-β, SMAD2, SMAD3, SMAD4, COL1A1, and COL3A1 were observed to be the highest in the 50–30 group, in comparison to the other three groups ($P < 0.5$, except for COL3A1 where no statistical difference was observed compared to the polished groups) (Fig. 3) (Table 4). In contrast, gene expression was significantly reduced in the 50–90 group and the 150–30 group compared to the polished group. Overall, these findings indicated that microtextured titanium sheets in the 50–30 group upregulated the expression of collagen-related genes, while microtextured titanium sheets that deviated from the cell size appeared to inhibit gene expression.

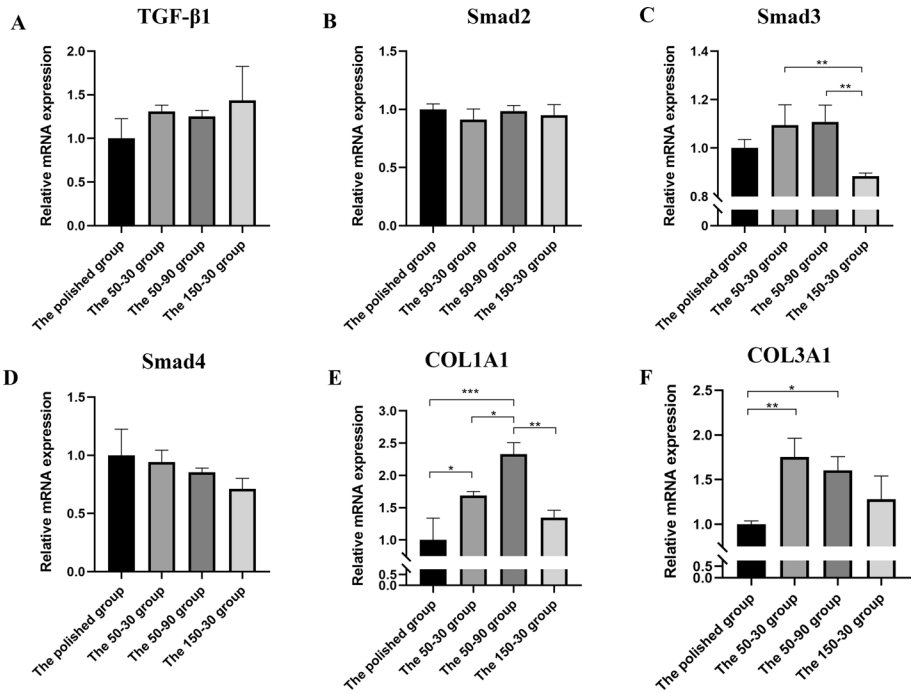

Fig. 2 Expression levels of collagen synthesis-related pathway genes in each group at day 4 of culture. *: $p < 0.05$. **: $p < 0.01$. ***: $p < 0.001$

Table 3 Expression levels of genes for collagen synthesis and its related pathways at day 4 of culture

	TGF-β_1	Smad2	Smad3	Smad4	COL1A1	COL3A1
Polished	1.0000 ± 0.2253	1.0000 ± 0.0472	1.0000 ± 0.0353	1.0000 ± 0.2241	1.0000 ± 0.3400	1.0000 ± 0.0357
50–30	1.3099 ± 0.0709	0.9113 ± 0.0914	1.0949 ± 0.0838	0.9436 ± 0.1012	1.6886 ± 0.0635	1.7521 ± 0.2102
50–90	1.2522 ± 0.0685	0.9861 ± 0.0475	1.1087 ± 0.0691	0.8541 ± 0.0366	2.3282 ± 0.1790	1.6036 ± 0.1536
150–30	1.4362 ± 0.3893	0.9508 ± 0.0901	0.8837 ± 0.0131	0.7103 ± 0.0918	1.3472 ± 0.1126	1.2797 ± 0.2597

Microfabricated titanium sheets significantly stimulated the secretion of collagen types I and III from mouse fibroblasts

To investigate collagen secretion in mouse fibroblasts, the expression of collagen I and III was analyzed using western blotting. On the fourth day, the expression of collagen I and III was significantly increased in both the 50–30 and 50–90 groups compared to the polished group (Fig. 4) (Table 5). On the seventh day, the 50–30 group exhibited the highest level of type I collagen expression, thereby confirming its superior ability to promote collagen secretion. Furthermore, the expression of collagen was found to be significantly higher in the 50–90 and 150–30 groups in comparison to the polished group. Notably, the 150–30 group exhibited the highest content of collagen III (Fig. 4) (Table 6). Although the expression of type III collagen in the 150–30 group was greater than that in the 50–30 group, it should be noted that type I collagen has a stronger tensile strength than type III collagen. As the process of tissue healing progresses, the expression of type III collagen is gradually replaced by that of type I collagen. This shift in expression results in a greater reliance on type I collagen for tensile strength maintenance. Consequently, it

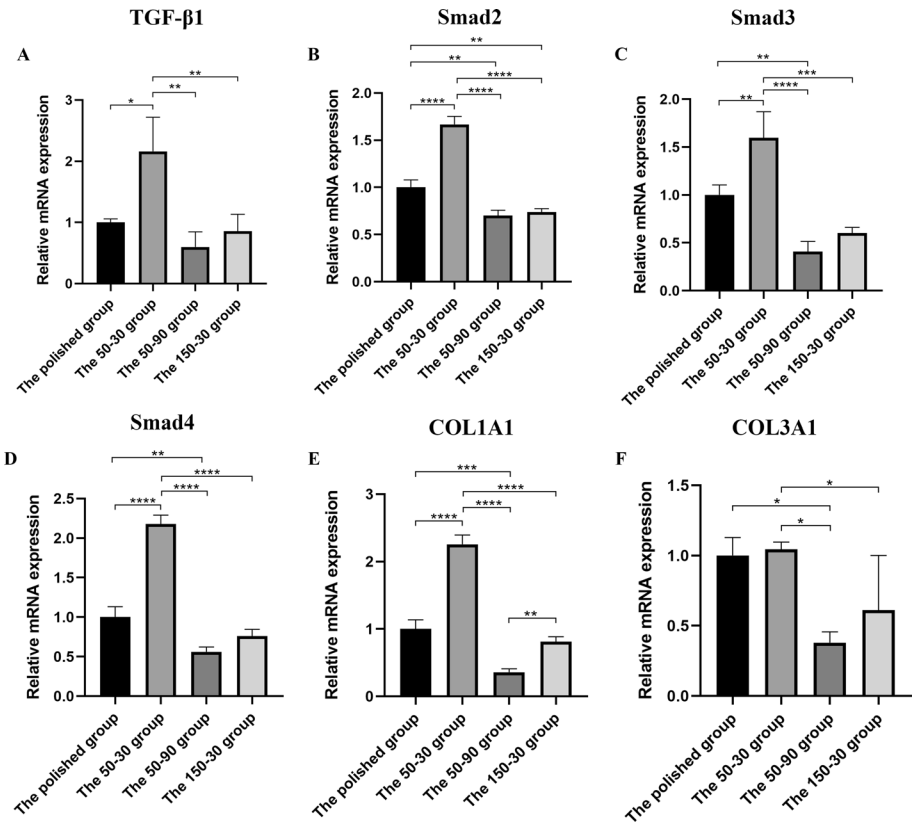

Fig. 3 Expression levels of collagen synthesis-related pathway genes in each group at day 7 of culture. *: $p < 0.05$. **: $p < 0.01$, ***: $p < 0.001$, ****: $p < 0.0001$

Table 4 Expression levels of genes for collagen synthesis and its related pathways at day 7 of culture

	TGF-β_1	Smad2	Smad3	Smad4	COL1A1	COL3A1
Polished	1.0000 ± 0.0591	1.0000 ± 0.0798	1.0000 ± 0.1038	1.0000 ± 0.1323	1.0000 ± 0.1370	1.0000 ± 0.1280
50–30	2.1610 ± 0.5588	1.6677 ± 0.0850	1.5959 ± 0.2737	2.1780 ± 0.1120	2.2573 ± 0.1368	1.0448 ± 0.0514
50–90	0.5984 ± 0.2472	0.7007 ± 0.0572	0.4100 ± 0.1036	0.5623 ± 0.0586	0.3585 ± 0.0498	0.3795 ± 0.0770
150–30	0.8555 ± 0.2772	0.7383 ± 0.0363	0.6012 ± 0.0601	0.7584 ± 0.0865	0.8103 ± 0.0744	0.6116 ± 0.3893

is of paramount importance to synthesize more type I collagen at this stage. These findings provided further evidence that microtextured surface might influence cell biology.

Discussion

In clinical practice, the materials most commonly used for gastrointestinal anastomotic staples are either pure titanium or titanium–nickel alloy. It has previously been demonstrated that the application of a chemical coating to the surface of the anastomosis can enhance the healing process [5, 6]. Nevertheless, there are limitations to this approach. One such limitation is the potential for the coating material to be released, which could result in a reduction in efficacy over time. Additionally, there is a possibility of resistance developing with long-term use. In an effort to overcome

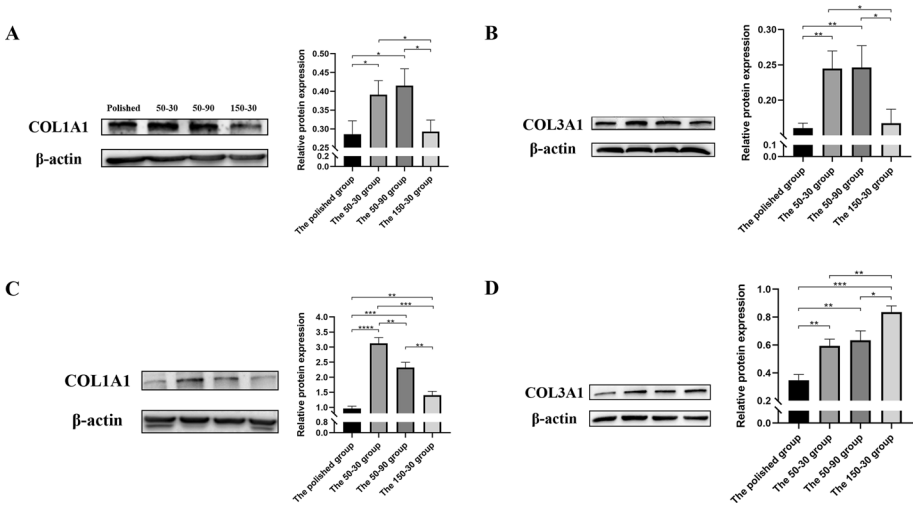

Fig. 4 Protein expression levels of collagen: **A** type I collagen at day 4; **B** type III collagen at day 4; **C** type I collagen at day 7; **D** type III collagen at day 7. *$p < 0.05$, **$p < 0.01$, ***$p < 0.001$, ****$p < 0.0001$

Table 5 Protein expression levels of type I collagen and type III collagen in each group at day 4 of incubation

	COL1A1	COL3A1
Polished	0.2858 ± 0.0356	0.1603 ± 0.0070
50–30	0.3910 ± 0.0372	0.2447 ± 0.0249
50–90	0.4149 ± 0.0450	0.2462 ± 0.0309
150–30	0.2930 ± 0.0305	0.1670 ± 0.0200

Table 6 Protein expression levels of type I collagen and type III collagen in each group at day 7 of incubation

	COL1A1	COL3A1
Polished	0.9633 ± 0.0742	0.3469 ± 0.0407
50–30	3.1254 ± 0.1913	0.5937 ± 0.0476
50–90	2.3207 ± 0.1750	0.6339 ± 0.0667
150–30	1.4061 ± 0.1269	0.8351 ± 0.0453

these shortcomings, we endeavored to physically transduce mechanical signals into biological electrical signals. The aim of this study was to design hexagonal microtextured surface on titanium sheets using a laser microtextured marking technology. We evaluated the proliferation of fibroblasts on the microtextured titanium sheets and assessed the expression of collagen types I and III. Our results indicated that laser microtextured titanium sheets surface significantly increased the roughness and reduced the contact angle, making them more hydrophilic. These surface modifications had a significant effect on promoting fibroblast proliferation and collagen type I and III secretion. Surface texturing designs have been found to have significant effects on cellular behavior at the genetic level [11–14]. In the field of bionics, certain natural

objects with unique surface morphologies have been found to have special properties. For example, the finger pads of tree frogs have excellent hydrophilicity and adhesion, allowing them to adhere effectively to various surfaces. Barnes et al. [15] observed that the surface microstructure of tree frog finger pads consists of dominant hexagonal prisms. According to the Wenzel model of wettability theory, the hexagonal prism structure offers the largest effective contact area and the best surface wettability compared to quadrangular, pentagonal, and heptagonal prisms. Moreover, the hexagonal prism structure and the grooves between them increase the effective solid–liquid contact area, resulting in high surface hydrophilicity and good adhesion [16]. The rate of cell growth and collagen aggregation are critical to tissue healing. In this study, we took inspiration from the surface microstructure of tree frog finger pads and constructed hexagonal prismatic micrometer-scale patterns with various sizes on titanium sheets. The aim of this study was to overcome the shortcomings of previous pure titanium and chemical coatings by converting mechanical signals on the surface of microtextured titanium sheets into bioelectrical signals in fibroblasts. Our results confirmed that the hexagonal microtextured surface of titanium sheets significantly promoted fibroblast growth. Compared to the polished group, both the 50–30 and 150–30 groups exhibited significant pro-proliferative effects, with the 50–30 group showing the most pronounced effect. The fibroblasts had a diameter range of approximately 17–20 μm, which closely matched with the size of the grooves between adjacent hexagonal prisms on the titanium sheet surface in the 50–30 group. As a result, the fibroblasts were able to better embed themselves in the grooves, thereby enhancing the biological effects of the textured surface on the cells. In addition, the 50–30 group showed superior hydrophilic properties, which may explain its stronger pro-proliferative effect on fibroblasts compared to the 150–30 group.

Type I collagen and type III collagen play a crucial role in maintaining the tensile strength of the anastomosis after gastrointestinal surgery [17]. Among the numerous secreted growth factors and cytokines, the transforming growth factor-β (TGF-β) family has been the subject of considerable research interest due to its multifaceted functions at the cellular level and during development, as well as its involvement in a wide range of diseases, including cancer [18]. Verrecchia et al. [19] observed that TGF-β promotes the healing of whole wounds and improves the strength of the wound tissue at an early stage of wound healing in a healing study of whole wounds in rabbit ears. In a separate study, coculturing adipose-derived stromal cells (ASCs) with bone marrow stromal cells (BMSCs) was observed to markedly enhance osteogenic differentiation and angiogenesis. Of particular note was the elevated level of transforming growth factor (TGF)-βR1 and SMAD3 observed in BMSCs cocultured with ASCs. These findings underscore the capacity of TGF-β to facilitate bone regeneration and tissue healing [20]. Research has shown that TGF-β1 can increase the expression of collagen synthesis-related genes, namely COL1A1 and COL3A1, through the TGF-β/Smad signaling pathway [21]. This leads to an increase in the levels of type I and type III collagen in the extracellular matrix, promoting tissue healing. In our study, we observed that hexagonal microtextured titanium sheets significantly activated the TGF-β/Smad signaling pathway and facilitated the expression of COL1A1 and COL3A1, which was consistent with previous research. Specifically, at day 4 of the culture, there were no significant differences in

gene transcript levels of the TGF-β1/Smad signaling pathway among the groups, except for Smad3. However, both the 50–30 and 50–90 groups exhibited higher levels of type I and type III collagen gene transcripts and protein expression. This suggested that these microtextured designs may promote early extracellular matrix production during the healing process. By day 7, the 50–30 group showed superior promotion of collagen synthesis at both the gene and protein levels, providing further evidence for the influence of hydrophilicity and the size of the microtextured structures on cellular responses. It is crucial to highlight that while the 150–30 group exhibited a higher level of type III collagen compared to the 50–30 group, it has been demonstrated that type I collagen exhibits superior tensile strength. As the process of tissue healing progresses, type III collagen is gradually replaced by type I collagen. Consequently, the synthesis of greater quantities of type I collagen at this stage is of greater importance for the maintenance of overall tensile strength.

Furthermore, it is essential to note that there is limited research dedicated to the enhancement of the surface morphology of titanium staples for gastrointestinal anastomosis through the promotion of tissue healing via surface texturing techniques. The results of our study indicated that the gene transcription of fibroblasts adhering to the surface of microtextured titanium sheets exhibited significant alterations. This suggested that surface-structured titanium sheets may have the potential to convert mechanical signals into biological ones. This provided a compelling rationale for the use of microtextured titanium sheets in promoting gastrointestinal tissue healing. The application of hexagonal prism-like textured titanium sheets on gastrointestinal anastomosis staples may prove beneficial in enhancing the healing of anastomotic tissues and improving patient prognosis. However, it is crucial to acknowledge the limitations of our work. Although the findings of our study indicated that hexagonal microtextured titanium sheets have a positive impact on fibroblast growth, further validation through in vivo experiments is necessary to confirm these results. Conducting long-term studies and in vivo evaluations is vital to assess their biocompatibility, mechanical stability, and potential clinical applications. Therefore, future investigations should include complementary in vivo experiments using animal models to verify the efficacy of microtextured titanium sheet anastomosis staples.

Conclusions

In this study, we employed laser microtextured marking technique to create hexagonal microtextured titanium sheets. The hexagonal microtextured surface displayed significant effectiveness in promoting the proliferation of mouse fibroblasts. Moreover, these microtextured titanium sheets exhibited the capability to activate the TGF-β/Smad signaling pathway, thereby inducing the synthesis of collagen type I and collagen type III. These findings indicated that the microtextured titanium sheets have the potential to facilitate tissue healing processes.

Materials and methods

Titanium sheet preparation and cell culture

Industrial pure titanium TA2 was procured from Angli Bearing Co. (Shanghai, China). Subsequently, cryopreserved mouse fibroblastic embryonic stem cells (NIH/3T3)

were thawed from the Institute of General Surgery, Tianjin Medical University. The NIH/3T3 cells were resuscitated and cultured on titanium sheets featuring distinct microtextured surface.

The TA2 pure titanium sheet, measuring 14 mm in diameter and 3 mm in thickness, underwent a metallographic grinding and polishing process using silicon carbide sandpaper with particle sizes of 400, 800, 1200, 1500, and 2000. Subsequently, three groups of hexagonal microtextured were created on the polished titanium sheets using the YLP-D20 laser marking machine (GBOS LASER INC. Dongguan, Guangdong, China) operating at a wavelength of 1064 nm. The laser settings included power of 4 W, 15 repetitions, and a speed of 100 mm/s. The three groups were distinguished by their microtextured parameters: 50 μm side length, 30 μm pitch, and 15 μm depth (denoted as 50–30); 50 μm side length, 90 μm pitch, and 15 μm depth (denoted as 50–90); and 150 μm side length, 30 μm pitch, and 15 μm depth (denoted as 150–30). The determination of these parameters was based on preliminary investigations conducted by our research group [22, 23]. Prior to subsequent experiments, the polished group was subjected to sequential immersion in acetone, ethanol, and deionized water, followed by ultrasonic cleaning for 10 min. This group was designated as the control, and four titanium sheets were assigned to each experimental group (Fig. 5).

The surface roughness of each titanium sheet was assessed using a handheld surface roughness meter (Taylor Hobson, UK), with measurements taken at five different locations on each sheet. The average value obtained from these measurements was considered as the average roughness (Ra) for each titanium sheet. Subsequently, droplets were applied to four distinct regions on the surface of the titanium sheet, and the contact angles at these locations were determined using the JC2000DM surface contact angle meter (Zhongchen Digital Technology Equipment Co. Shanghai,

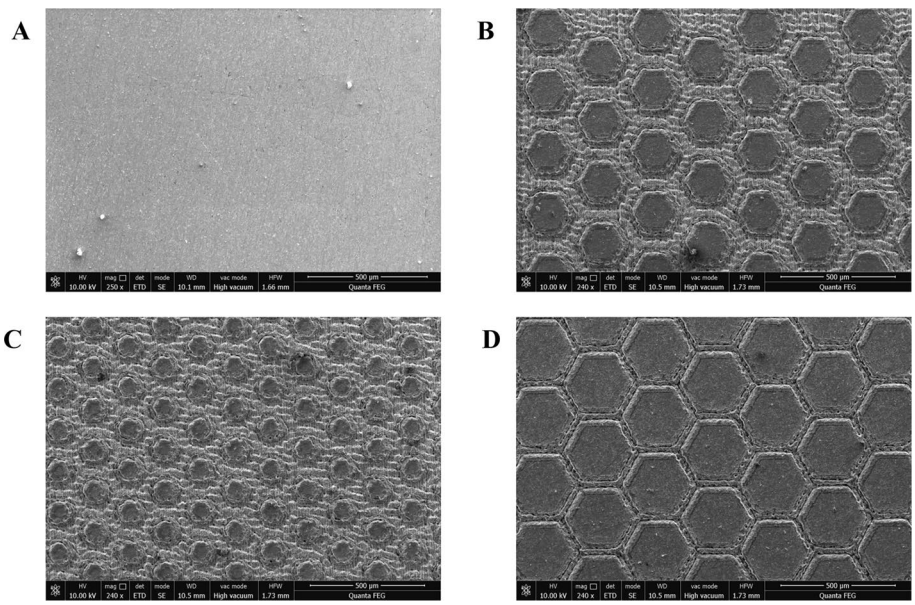

Fig. 5 Hexagonal microtextured titanium sheet surfaces produced with varying parameters using a laser marking machine: **A** polished; **B** 50–30; **C** 50–90; **D** 150–30

China). The average contact angle obtained from these measurements represented the contact angle of the titanium sheet's surface.

Mouse fibroblasts NIH/3T3 were routinely cultured at the Institute of General Surgery, General Hospital of Tianjin Medical University. Prior to cell inoculation, 3–5 cell passages were performed. The previously prepared titanium sheets were carefully placed into 24-well plates. The cell density was adjusted to $1\times10^{\wedge4}$ /ml. After mixing the cell suspension, 1 ml was added to each well and used for subsequent experiments.

CCK8 assay

To determine the viability of cells, CCK8 assay was performed using CCK8 detection kit (Suolaibao Technology Co. Ltd. Beijing, China) according to the instruction of the Kit. The NIH/3T3 cells ($1\times10^{\wedge4}$ /well) were seeded in 24-well plates at 37 ℃ with 5% CO_2. After incubation for 0, 48, 96 and 144 h, CCK-8 solution (100 μL) was added to each well, after which cells were incubated for 2 h. Then, 100 μl of culture supernatant was added carefully to a 96 plate and the optical density (OD) was read at 450 nm using the microplate reader (TECAN microplate reader, Molecular Devices, Austria). Each sample was added to 3 wells and the average value was taken as the final OD. The value of OD 450 nm represents the viability of cells.

qRT-PCR

The expression levels of secreted collagen-related genes on fourth and seventh day were determined through qRT-PCR, including transforming growth factor beta 1 (TGF-β1), SMAD family member 2, 3, 4 (Smad2, 3, 4), Collagen Type I Alpha 1 Chain (COL1A1), and Collagen Type III Alpha 1 Chain (COL3A1). Prior to performing qRT-PCR, TRIZOL (Invitrogen) was used to lyse fresh NIH/3T3 cells and to protect total RNA from degradation. Then, complementary DNA (cDNA) was synthesized using a HiScript® III 1st Strand cDNA Synthesis Kit (+gDNA wiper) (Nanjing Nuoweizan Biological Technology Co. Ltd. China). Then, qRT-PCR analysis was performed using the SYBR qPCR Master Mix (Nanjing Nuoweizan Biological Technology Co. Ltd. China). All samples were performed with the BioRad CFX96 (Bio-Rad, USA). Primer sequences are listed below in Table 7.

Table 7 Primer sequences

Primer	Forward (5′-3′)	Reverse (5′-3′)
TGF-β1	ACTGGAGTTGTACGGCAGTG	GGGGCTGATCCCGTTGATTT
Smad2	AAGCCATCACCACTCAGAATTG	CACTGATCTACCGTATTTGCTGT
Smad3	CACGCAGAACGTGAACACC	GGCAGTAGATAACGTGAGGGA
Smad4	ACACCAACAAGTAACGATGCC	GCAAAGGTTTCACTTTCCCCA
COL1A1	TAAGGGTCCCCAATGGTGAGA	GGGTCCCTCGACTCCTACAT
COL3A1	ACGTAGATGAATTGGGATGCAG	GGGTTGGGGCAGTCTAGTG
GAPDH	AATGGATTTGGACGCATTGGT	TTTGCACTGGTACGTGTTGAT

Western blot

To determine collagen expression as previously described, western blots were performed according to the manufacturer's recommendations. After incubation for 96 h and 168 h, cell samples were homogenized in RIPA lysis buffer (Suolaibao Technology Co. Ltd. Beijing, China) and further centrifuged at 14,000 *g* at 4 ℃ for 30 min. Prior to electrophoresis, protein concentration of each sample was determined by BCA assay using the BCA kit (Suolaibao Technology Co. Ltd. Beijing, China) according to manufacturer's instructions. Equal amounts of protein (20 μg) were loaded onto 8% SDS-PAGE gel, then electrophoresed and transferred to a polyvinylidene fluoride (PVDF) membrane. Then the PVDF membrane was put gently into 5% non-fat blocking grade milk to block one hour and incubated with the COL1A1 and COL3A1 primary antibodies (1:1000) overnight at 4 ℃. On the following day, the membranes were incubated with the appropriate secondary antibody (1:5000) at room temperature for 1 h. Then protein was visualized by ECL kit (Suolaibao Technology Co. Ltd. Beijing, China) according to manufacturer's instructions. Immunoblot signals were quantified using ImageJ. The results were normalized using β-actin as an internal control.

Statistics analysis

Statistical analysis was conducted using GraphPad Prism 8.0.2 software (GraphPad Software, Inc., USA). Group comparisons were made using one-way ANOVA, while unpaired t-tests were employed for two-way comparisons between groups. $P < 0.05$ was considered statistically significant.

Provenance and peer review

Not commissioned, externally peer-reviewed

Supplementary Information

The online version contains supplementary material available at https://doi.org/10.1186/s12938-024-01313-0.

Supplementary material 1.

Supplementary material 2.

Acknowledgements

Assistance with the study: The authors would like to thank Tianjin Medical University General Hospital, Fundamental Research Cooperation Program of Beijing–Tianjin–Hebei Region of Natural Science Foundation of Tianjin, Tianjin Major Science and Technology Project, Tianjin Key Medical Discipline (Specialty) Construction Project, Health Science and Technology Project of Tianjin Health Commission and Tianjin Medical University for support. Presentation: None

Author contributions

H H, Y H and W F contributed to the conception and design of the study. R F fabricated the microtextured titanium sheets used in this experiment. H H, P W, Z L and Q S completed the biology experiment. R F and Z L carried out the processing of the image. P W, Z L and B L performed the statistical analysis. H H wrote the first draft of the manuscript. Y H and W F wrote sections of the manuscript. All authors contributed to manuscript revision and read and approved the submitted version.

Funding

This study was supported by grants from Fundamental Research Cooperation Program of Beijing–Tianjin–Hebei Region of Natural Science Foundation of Tianjin (22JCZXJC00140), Tianjin Major Science and Technology Project (21ZXJBSY00110), Tianjin Health, Science and Technology Project (TJWJ2024ZK001) and Tianjin Key Medical Discipline (Specialty) Construction Project (TJYXZDXK-005A).

Availability of data and materials

All data, materials, and operation videos used during the study are available from the corresponding author by request.

Declarations

Consent for publication
Not applicable.

Competing interests
The authors declare no competing interests.

Received: 27 July 2024 Accepted: 7 November 2024
Published online: 22 November 2024

References

1. Chiarello MM, Fransvea P, Cariati M, Adams NJ, Bianchi V, Brisinda G. Anastomotic leakage in colorectal cancer surgery. Surg Oncol. 2022;40: 101708.
2. Su EP, Justin DF, Pratt CR, Sarin VK, Nguyen VS, Oh S, et al. Effects of titanium nanotubes on the osseointegration, cell differentiation, mineralisation and antibacterial properties of orthopaedic implant surfaces. Bone Joint J. 2018. https://doi.org/10.1302/0301-620X.100B1.BJJ-2017-0551.R1.
3. Zhu Y, Liu D, Wang X, He Y, Luan W, Qi F, et al. Polydopamine-mediated covalent functionalization of collagen on a titanium alloy to promote biocompatibility with soft tissues. J of materials chemistry B. 2019;7(12):2019–31.
4. Wang PH, Huang BS, Horng HC, Yeh CC, Chen YJ. Wound healing. J Chin Med Assoc. 2018;81(2):94–101.
5. Wang Y, Cai X, Mei J, Liu K, Cai X. Colonic anastomosis with a doxycycline-coated stent: an experimental study in a porcine model. Dig Surg. 2014;31(2):87–94.
6. Chua PH, Neoh KG, Shi Z, Kang ET. Structural stability and bioapplicability assessment of hyaluronic acid-chitosan polyelectrolyte multilayers on titanium substrates. J Biomed Mater Res. 2008;87(4):1061–74.
7. Enezei HH, Ahmad A, Takeuchi K, Suzuki J, Khamis MF, Razak NHA, et al. Osteoinductive activity of bone scaffold bioceramic companied with control release of VEGF protein treated dental stem cells as a new concept for bone regeneration. J Hard Tissue Biol. 2018. https://doi.org/10.2485/jhtb.27.69.
8. Qabbani Al, Kawas Al, Noor H, Razak SW, Bayatti Al, Enezei HH, Rani Samsudin A, et al. Three-dimensional radiological assessment of alveolar bone volume preservation using bovine bone xenograft. J Cranio Surg. 2018. https://doi.org/10.1097/SCS.0000000000004263.
9. Hori N, Iwasa F, Ueno T, Takeuchi K, Tsukimura N, Yamada M, et al. Selective cell affinity of biomimetic micro-nano-hybrid structured TiO2 overcomes the biological dilemma of osteoblasts. Dental Mater. 2010;26(4):275–87.
10. Morikawa M, Derynck R, Miyazono K. TGF-β and the TGF-β Family: Context-dependent roles in cell and tissue physiology. Cold Spring Harbor Perspect biol. 2016. https://doi.org/10.1101/cshperspect.a021873.
11. Chen W, Villa-Diaz LG, Sun Y, Weng S, Kim JK, Lam RH, et al. Nanotopography influences adhesion, spreading, and self-renewal of human embryonic stem cells. ACS Nano. 2012;6(5):4094–103.
12. Ding Y, Sun J, Ro HW, Wang Z, Zhou J, Lin NJ, et al. Thermodynamic underpinnings of cell alignment on controlled topographies. Adv Mater. 2011;23(3):421–5.
13. Wu YN, Law JB, He AY, Low HY, Hui JH, Lim CT, et al. Substrate topography determines the fate of chondrogenesis from human mesenchymal stem cells resulting in specific cartilage phenotype formation. Nanomed Nanotechnol Biol Med. 2014;10(7):1507–16.
14. Kwon KW, Park H, Song KH, Choi JC, Ahn H, Park MJ, et al. Nanotopography-guided migration of T cells. J Immunol. 2012. https://doi.org/10.4049/jimmunol.1102273.
15. Barnes WJ, Baum M, Peisker H, Gorb SN. Comparative Cryo-SEM and AFM studies of hylid and rhacophorid tree frog toe pads. J Morphol. 2013;274(12):1384–96.
16. Langowski JKA, Dodou D, Kamperman M, van Leeuwen JL. Tree frog attachment: mechanisms, challenges, and perspectives. Front Zool. 2018;15:32.
17. Witte MB, Barbul A. General principles of wound healing. Surg Clin North Am. 1997;77(3):509–28.
18. Jaggessar A, Shahali H, Mathew A, Yarlagadda P. Bio-mimicking nano and micro-structured surface fabrication for antibacterial properties in medical implants. J Nanobiotechnol. 2017;15(1):64.
19. Verrecchia F, Mauviel A. TGF-beta and TNF-alpha: antagonistic cytokines controlling type I collagen gene expression. Cell Signal. 2004;16(8):873–80.
20. Kim KI, Park S, Im GI. Osteogenic differentiation and angiogenesis with cocultured adipose-derived stromal cells and bone marrow stromal cells. Biomaterials. 2014;35(17):4792–804.
21. Raghu G, Masta S, Meyers D, Narayanan AS. Collagen synthesis by normal and fibrotic human lung fibroblasts and the effect of transforming growth factor-beta. Am Rev Respir Dis. 1989;140(1):95–100.
22. Hu Y, Duan J, Yang X, Zhang C, Fu W. Wettability and biological responses of titanium surface's biomimetic hexagonal microstructure. J Biomater Appl. 2023;37(6):1112–23.
23. Zhang Z, Li Y, Zhang T, Yang X, Fan K, Wang D, et al. Titanium implants modified by laser microtexturing enhance the bioactivity of gastric epithelial cells and fibroblast cells. J Appl Biomater Funct Mater. 2021;19:22808000211064950.

Publisher's Note